In vivo Effects of Temperature on the Heart and Pyloric Rhythms in the Crab, *Cancer borealis*.

Dahlia Kushinsky*#, Ekaterina O. Morozova* and Eve Marder
Biology Department and Volen Center
Brandeis University
Waltham, MA 02454

#present address: Weizmann Institute of Science, 234 Herzl Street, Rehovot, Israel

*these authors contributed equally

Corresponding author email – marder@brandeis.edu

Running title: *In vivo* heart and pyloric rhythms

Key words – photoplethysmography, crustaceans, stomatogastric nervous system, cardiac ganglion, central pattern generators, Q_{10}

Author Contributions: Experiments and design, D.K.; data analysis and figure preparation, D.K. and E.O.M. Manuscript writing and editing, D.K., E.O.M. and E.M.

Summary Statement

Temperature elevation increases the frequency of the heart and pyloric rhythms of the crab, *Cancer borealis,* but the heart rhythm has a higher critical temperature than the pyloric rhythm.

Abstract

The heart and pyloric rhythms of crustaceans have been studied separately and extensively over many years. Local and hormonal neuromodulation and sensory inputs onto these central pattern generating circuits play a significant role in the animals' responses to perturbations, but are usually lost or removed during *in vitro* studies. To examine simultaneously the *in vivo* motor output of the heart and pyloric rhythms, we used photoplethysmography (PPG). In the population measured (n = 49), the heart rhythm frequencies ranged from 0.3-2.3 Hz. The pyloric rhythms varied from 0.2-1.6 Hz. During multiple hour-long recordings, many animals held at control temperature showed strong inhibitory bouts in which the heart decreased in frequency or become quiescent and the pyloric rhythm also decreased in frequency. Many animals show significant coherence in frequency between the rhythms at the frequency of the heart rhythm. We measured the simultaneous responses of the rhythms to temperature ramps by heating or cooling the saline bath while recording both the heart and pyloric muscle movements. Q_{10}s, critical temperatures (temperatures at which function is compromised), and changes in frequency were calculated for each of the rhythms tested. The heart rhythm was more robust to high temperature than the pyloric rhythm.

42 **Introduction**

43 Central pattern generators (CPGs) are responsible for the generation of many
44 rhythmic motor patterns that are vital for muscle movements of an animal's life. In
45 crustaceans, mechanisms of central pattern generation have been studied using the
46 cardiac ganglion (CG), which produces heart movements, and the stomatogastric
47 ganglion (STG) which generates the rhythmic movements of the stomach (Cooke, 2002;
48 Maynard, 1972). These two rhythms are subject to both local and global modulation.
49 These rhythms have been studied separately, both *in vivo* and in dissected and isolated
50 preparations, but now we ask whether these rhythms appear to be coordinated in an
51 intact animal.

52 The heart of the crustacean is neurogenic, controlled by motor neuron discharges
53 produced by the CG. In normal conditions, the heart continuously pumps hemolymph
54 through an open circulatory system to distribute oxygen and neuromodulators to the
55 animal's tissues (McMahon, 1995; McMahon, 2001a; McMahon, 2001b). This
56 circulatory system is formed by elaborate capillary beds in many of the animal's tissues,
57 paired with valves that allow for selective hemolymph distribution (McMahon, 1995;
58 McMahon, 2001a; McMahon, 2001b). The cardiac output, calculated as the stroke
59 volume/heart rate, must be maintained to ensure adequate hemolymph distribution
60 (McGaw and McMahon, 1996). Hemolymph flow rate and stroke volume are subject to
61 wide variations both within and across animals (McGaw and McMahon, 1996). Changes in
62 flow rate are likely due to modifications in stroke volume or valve activation, and may
63 occur in response to local tissue demands (McGaw and McMahon, 1996; Wilkens and
64 McMahon, 1994). Changes in cardiac output may also be the result of spontaneous firing

events in the CNS, CG, or cardioarterial valves of the heart (McGaw and McMahon, 1996; Wilkens and McMahon, 1994).

The CG, controlling the movement of the heart, contains an intrinsically oscillating pacemaker to form a central pattern generated rhythm. Additionally, the heart is innervated by extrinsic fibers, one inhibitory and two excitatory, that modify heart rate in relation to behavioral demands (Cooke, 2002). The CG of the crab, *Cancer borealis,* is comprised of nine neurons, 4 small and 5 large cells, that burst in time to produce muscle movements. The CG also produces patterned bursts of impulses in response to simple stimuli, such as excitation from stretch sensitive dendrites (Cooke, 2002). This allows the heart to adjust its frequency and strength of contractions when faced with different metabolic needs (Dickinson et al., 2016a; Dickinson et al., 2015a).

The stomatogastric nervous system (STNS) has long been used to study central pattern generation and mechanisms underlying rhythmic and continuous motor patterns (Maynard, 1972). The STNS controls the movement of the crustacean stomach (Maynard and Dando, 1974; Morris and Hooper, 1997; Morris and Hooper, 1998; Morris and Hooper, 2001). Foregut movements allow for feeding behavior, including chewing, swallowing, and processing of waste (Clemens et al., 1998b; Johnson and Hooper, 1992). Oxygen tension alters the neuronal activity of the STG and therefore its motor output (Clemens et al., 2001). The stomach is a complex mechanical structure with ossicles that provide mechanical support and insertions for intrinsic stomach muscles (Maynard and Dando, 1974). The STNS generates the continuously active and rapid pyloric rhythm and the slower, episodic gastric mill movements (Clemens et al., 1998a; Clemens et al., 1999; Clemens et al., 1998b; Clemens et al., 2001; Clemens et al.,

88 1998c; Heinzel, 1988; Heinzel and Selverston, 1988; Rezer and Moulins, 1983; Soofi et
89 al., 2014).

90 The pericardial organs (POs) are secretary organs that deliver neurohormones to
91 the animal's hemolymph (Alexandrowicz and Carlisle, 1953; Chen et al., 2010; Christie
92 et al., 1995; DeKeyser et al., 2007; Hui et al., 2012). These neuromodulators may
93 increase the frequency and amplitude of the heartbeat (Christie et al., 2008; Cruz-
94 Bermudez and Marder, 2007; Sullivan and Miller, 1984; Williams et al., 2013), or
95 change the frequency of the pyloric rhythm (Hooper and Marder, 1987; Marder, 2012;
96 Marder and Bucher, 2007). Hemolymph containing neuromodulators flows into the
97 heart and is pumped throughout the open circulatory system, filling the ophthalmic
98 artery, directly bathing the STG. The modulators released into the hemolymph act
99 hormonally, and therefore may affect the animal's various organs in the same manner,
100 or may have varied effects depending on the receptors present in the tissues. This
101 provides a feedback system within the animal, allowing for the simultaneous adjustment
102 of organ activity when needed in the animal.

103 Throughout its life, an organism must respond to perturbations that affect the
104 nervous system and the biomechanical structures it controls. Crustaceans are
105 poikilotherms and therefore may experience wide variations in body temperature due to
106 temperature changes in the environment. Because of this, it is relevant to study the
107 effect of temperature on the activity of the STNS and CG, as temperature changes may
108 simultaneously affect cellular processes of both systems and disrupt neuronal function.
109 Throughout their lives, crustaceans experience both short term temperature
110 fluctuations, due to changing tidal patterns during a single day, and long term

111 temperature fluctuations, due to seasonal temperature variations (Soofi et al., 2014;
112 Tang et al., 2010; Tang et al., 2012). Despite these varied temperature changes, animals
113 must maintain rhythmicity and performance of the foregut and heart. Therefore,
114 temperature is a useful manipulation to study network stability in the face of
115 perturbation.

116 Previous work on crustaceans indicate that both the heart and pyloric rhythms
117 are robust to temperature changes. In the heart, studies have shown that the strength of
118 a heartbeat decreases and heart rate increases with increases in temperature (Camacho
119 et al., 2006; Worden et al., 2006). Therefore, the increase in heart rate partially
120 compensates for the decrease in stroke volume as the CG is further pushed from its
121 normal state at 11°C. The pyloric triphasic rhythm is maintained across a wide range of
122 temperatures. In both the heart and the pyloric rhythm, the maximum frequency
123 attained at highest temperatures *in vivo* are lower than those of *in vitro* conditions,
124 likely due to the presence of sensory feedback and neurohormonal input (Soofi et al.,
125 2014; Worden et al., 2006).

126 The Q_{10} is a measure of the sensitivity of a biological process to a 10°C change in
127 temperature. Many biological processes have Q_{10}s between two and three, while some
128 temperature sensitive ion channels have Q_{10}s as high as 50 or 100 (Marder et al., 2015).
129 If all Q_{10}s of the components involved in a biological process are similar, this process is
130 likely to be temperature compensated (Caplan et al., 2014; Marder et al., 2015; O'Leary
131 and Marder, 2016; Robertson and Money, 2012). In both the heart and pyloric rhythms,
132 the Q_{10}s for the rhythm frequencies are similar *in vivo* and *in vitro* (Soofi et al., 2014;
133 Worden et al., 2006). Worden and colleagues (2006) noted that in the heart, the Q_{10}s of

various parameters were 1- 3.5. The pyloric rhythm increases in frequency with Q_{10}s between 2 and 2.5 while conserving its phase relationships within the triphasic rhythm (Soofi et al., 2014; Tang et al., 2010).

Temperature increases beyond 23°C lead to severely disrupted motor patterns and subsequent loss of rhythms in the heart and pyloric rhythms (Rinberg et al., 2013; Tang et al., 2012). Recordings of the pyloric rhythm show that preparations appear similar at permissive temperatures, but extreme temperatures disrupt, or crash them, in dissimilar ways revealing their variability (Marder et al., 2015; Rinberg et al., 2013; Tang et al., 2012).

In this study we systematically explore the potential relationships between stomach and heart rhythms, and ask whether they are coordinately sensitive to perturbation by temperature.

148 **Materials and Methods**

149 Animals

150 Adult male Jonah crabs (*Cancer borealis)* between 400 and 700 grams were
151 obtained from Commercial Lobster (Boston, MA). Animals were housed in tanks with
152 artificial seawater (Instant Ocean) between 10°C and 13°C on a 12 hour light/dark cycle
153 without food for a maximum of 10 days. For *in vivo* experiments, animals were placed in
154 a 25 liter tank filled with approximately 10 liters of artificial seawater inside an
155 incubator at 10°C to 12°C. Experiments were done between 9/1/16 and 7/12/17.

156 Prior to each experiment, crabs were weighed and anesthetized on ice for 10
157 minutes. Photoplesmogram (PPG) sensors (Vishay CNY70331) (Fig. 1), as described in
158 Depledge (1983), were placed on the carapace above the heart and pyloric muscles to
159 record the heart and pyloric rhythms, respectively. Sensors were secured to the carapace
160 using dental wax and cyanoacrylate glue (Starbond, EM-2000) and covered in Marine
161 Adhesive Sealant (3M, Fast Cure 5200) to waterproof and ensure the stability of the
162 sensors over time. After the sensors were attached to the animal, we waited a minimum
163 of 16 hours prior to experimental recordings, during which time the animals were not
164 handled and the door to the incubator was not opened.

165 Temperature Experiments

166 After a period of baseline (10°C to 12°C) recording, water temperature was
167 manipulated by flowing either cold or warm saline into the tank through a tube inserted
168 through the door of the incubator. A vacuum line was used to pump water out of the
169 tank to maintain a constant volume. Temperature was slowly ramped from 11°C to 32°C
170 over 1.5 to 2 hours. Heart rate was closely monitored to ensure health during the

171 temperature changes and ramps were halted once the heart rate developed an
172 arrhythmia or decreased to baseline frequencies, indicating that a 'critical temperature'
173 had been reached. Increasing temperatures past this critical temperature lead to death
174 of the animal, as the heart no longer recovered functionality.

175 Data Acquisition and Analysis

176 PPG data were acquired through the PPG amplifier (Newshift AMP03) and
177 recorded digitally through a digitizer (Axon Digidata 1550B) into computer software
178 (AxoScope 10.6) with a sampling frequency of 500 Hz. Data were analyzed using custom
179 written C and MATLAB codes.

180 Analysis of heart rhythm frequency

181 Heart rhythm frequency was calculated as the frequency at the peak spectral
182 power. We used the Burg (1967) method to estimate the power spectrum density at each
183 moving-time window. The Burg method (1967) fits the autoregressive (AR) model of a
184 specified order p in the time series by minimizing the sum of squares of the residuals.
185 The fast-Fourier transform (FFT) spectrum is estimated using the previously calculated
186 AR coefficients. This method is characterized by higher resolution in the frequency
187 domain than traditional FFT spectral analysis, especially for a relative short time
188 window (Buttkus, 2000). We used the following parameters for the spectral estimation:
189 data window of 12.8 s (128 samples), 50% overlap to calculate spectrogram, number of
190 estimated AR-coefficients p=window/4+1. Before the analysis, the voltage offsets of the
191 PPG recordings were removed, low pass filtered to 5 Hz using six-order Butterworth
192 filter and downsampled. Average baseline frequencies of heart rhythm were calculated
193 as median frequencies at peak of the power spectral density for each window of a
194 spectrogram during baseline conditions. Cumulative histograms of baseline frequencies

195 were calculated as a sum of histograms from individual animals normalized so that the
196 sum of bar heights is less than or equal to 1.

197 Analysis of the pyloric rhythm frequency

198 The pyloric rhythm frequency was calculated in a similar way as the heart
199 frequency in those cases that showed no interference from heart activity. However, there
200 were instances in which the heart activity was influencing the pyloric rhythm. This was
201 obvious in the pyloric rhythm spectrogram as a peak in the power spectrum density at
202 the frequency of heart rhythm. To identify the intrinsic frequency of the pyloric rhythm
203 in cases with heart interference, a linear regression model was fit to the pyloric signal
204 taking into account the phase difference between the heart and pyloric signals. The
205 heart signal was multiplied by the coefficients of the regression model and subtracted
206 from the pyloric signal. Then spectrogram of the subtracted signal was calculated, and
207 the pyloric frequency was identified as the frequency at peak spectral power. In some
208 cases, the pyloric rhythm frequency could not be determined due to irregularities in the
209 signal.

210 Analysis of the inhibitory bouts

211 We used a hidden Markov model (HMM) to infer the active and inhibitory states
212 of heart rhythms. In HMM, a timeseries is modeled as being generated probabilistically
213 from an underlying discrete-valued stochastic process (Rabiner, 1989). The data can be
214 either discrete- or continuous-valued, while the unobservable 'hidden' state is a discrete
215 random variable that can take *n* possible values (in our case n=2, representing active
216 and inhibitory states). Estimation of the transition probabilities for HMM was done
217 using the Baum-Welch algorithm, which utilizes an expectation maximization (EM)
218 algorithm (Bilmes, 1998) . The initial parameters used for the detection: transition

matrix $P_{AI} = P_{IA} = 0.9$, $P_{AA} = P_{II} = 0.1$, where P_{AI} is transition probability from active to inhibitory state, P_{AI} is a transition probability from inhibitory to active state, P_{ii} is a transition probability from inhibitory to inhibitory state and P_{AA} is a transition probability from active to active state. Identification by HMM states was used to calculate the durations of active and inhibitory bouts of heart rhythm.

Coherence analysis

Coherence between heart and pyloric data was calculated with multi-taper Fourier analysis (Mitra et al., 1999) using Chronux toolbox (htpp://www.chronux.org). Data were binned into two-minute bins, moved in 5 second steps. The time-bandwidth product was set to 10, and 19 tapers were used. Peak coherence and frequency of peak coherence were calculated for each window. The theoretical confidence level of the coherence was calculated as following:

$$ConfC = \sqrt{1 - p^{df}}, df = \frac{1}{dof / 2 - 1}$$

where dof is degrees of freedom. Based on these calculations, coherence values > 0.625 reached the significance of $p < 0.05$ with a Bonferroni correction. Data sets that had significant coherence more 50% of time during baseline were considered to have significantly coherent heart and pyloric rhythms and were calculated for each data set. The phase difference between the heart and pyloric rhythms was calculated at the frequency of the peak coherence for each window and median value of phase difference was reported for each dataset with significantly coherent signals.

Q_{10} estimation

We estimated the Q_{10} of frequency of the heart and pyloric rhythms *in vivo*. Frequency (Fr) of the heart and pyloric rhythms were plotted as a function of

temperature (T) in a logarithmic scale, and the Q_{10} was extracted from the slope of the linear regression (m) following the equation:

$$Q_{10} = 10^{10m}, m = \frac{d\log_{10}(\mathrm{Fr})}{dT}$$

The goodness of fit of the linear regression model for each dataset was assessed by calculating the coefficient of determination R^2, calculated as R^2 = (correlation coefficient)^2. We report R^2 for heart and pyloric data in the tables below. For majority of the fits we obtained high values of $R^2 > 0.8$.

Table 1. Statistics for heart frequency dependence on temperature.

R^2 for heart frequency vs T fit	R^2 for pyloric frequency vs T fit
0.921	
0.773	
0.792	
0.589	0.956
0.486	0.332
0.9052	0.8536
0.9085	0.933
0.9618	0.789
0.98	0.9871
0.996	
0.81	0.8691

Critical Temperature Analysis

The critical temperature was defined as the temperature at which the heart and pyloric movements became irregular and the frequency of muscle contraction significantly dropped. This was determined from the spectrograms of heart and pyloric rhythms. In some cases, the critical temperature of the pyloric rhythm was impossible to determine due to irregularity in pyloric rhythm signal.

Statistical analysis

All statistical analyses were done in Matlab. Between group comparisons were done using one-way ANOVA. Significance level was set to 0.05. When appropriate Bonferroni corrections were implemented.

Results

Heart and pyloric muscle movements of *Cancer borealis* were recorded *in vivo* using photoplesmography (PPG) (Fig. 1). In most of the experiments described, both rhythms were recorded from the same animals, although in some only the heart rhythms were recorded. It is straightforward to place a PPG sensor over the heart because the heart is dorsal, and situated just under the carapace, and its movements are large and vigorous, almost in the same plane as the sensor itself. The dorsal artery exits the heart and travels anteriorly close to the surface of the stomach. The pylorus is the most posterior region of the stomach, but most of its movements are in the interior of the animal. The thin straps of the dorsal dilator muscles of the pyloric region connect the pylorus to insertions just below the carapace, and the movements of these muscles are almost orthogonal to the carapace. Therefore, picking up these movements is considerably more difficult than those of the heart. Each heart beat would lead to a pressure wave in the artery, and the artery runs close to the dorsal dilator muscles, so it is to be expected that the pyloric PPG sensor might pick up some trace of the heart rhythm.

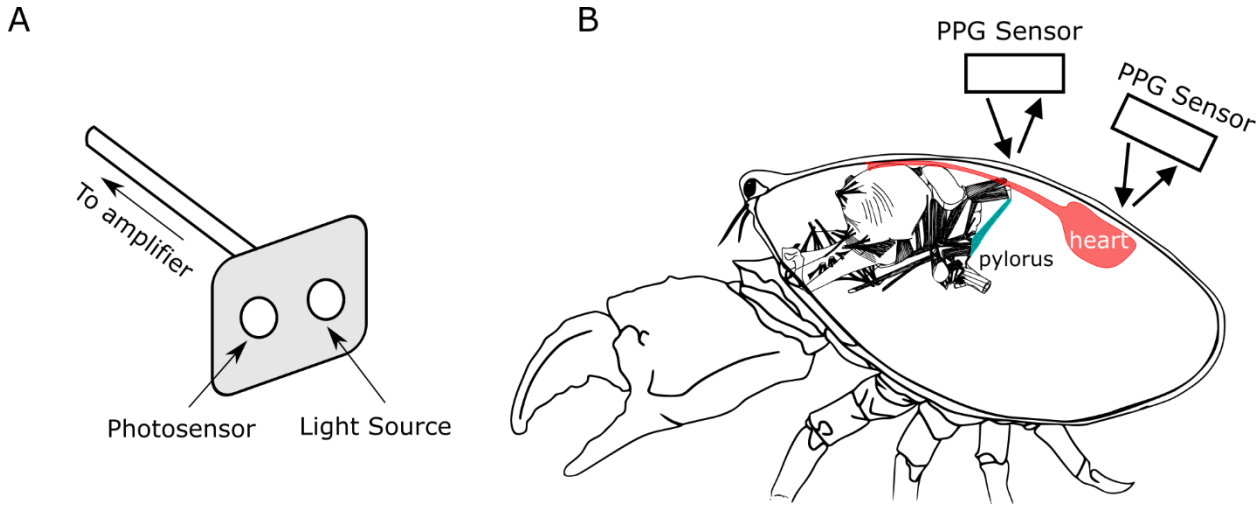

Figure 1. **Use of photoplesmography (PPG) allows for continuous noninvasive recordings of the heart and pyloric muscles**. **A)** Drawing of PPG sensor system, indicating light source and photosensor on device. **B)** Drawing of the PPG sensor positioning for detection of heart and pylorus movements when placed on the carapace of an animal. Infrared light from the sensors is emitted and travels through the animal's carapace before being reflected from the muscle directly below the PPG sensor. Crab image modified from http://stg.rutgers.edu/Resources.html. Stomach image was modified from Maynard and Dando, (1974).

Figure 2 shows sample recordings and spectrograms calculated from them for both the heart and pyloric rhythms. Figure 2A (left) shows three short stretches of raw data from 3 crabs; animal 1 had a relatively slow and steady heart rhythm (0.6 Hz), animal 2 had a relatively high frequency (1.1 Hz) and steady heart rhythm, and animal 3 showed a rhythm that switched from high to low frequency spontaneously, and then from low to high frequency in response to a saline injection. To the right of each of the sets of raw traces there is a spectrogram showing 1-2 hours of recordings, with the location of each of the raw data indicated.

Recordings of the pyloric rhythm with PPGs yielded complex, highly variable waveforms due to the angle of the dorsal dilator muscle movement with respect to the PPG sensor placement on the carapace of the animal. Figure 2B shows raw trace plesmograph recordings and their associated spectrograms of the pyloric rhythms from two animals. Animal 4 maintained a stable frequency of pyloric rhythm, while animal 5 showed a more variable rhythm during its baseline period. The frequency of the pyloric rhythm tends to decrease in response to saline injection as in the spectrogram for animal 5.

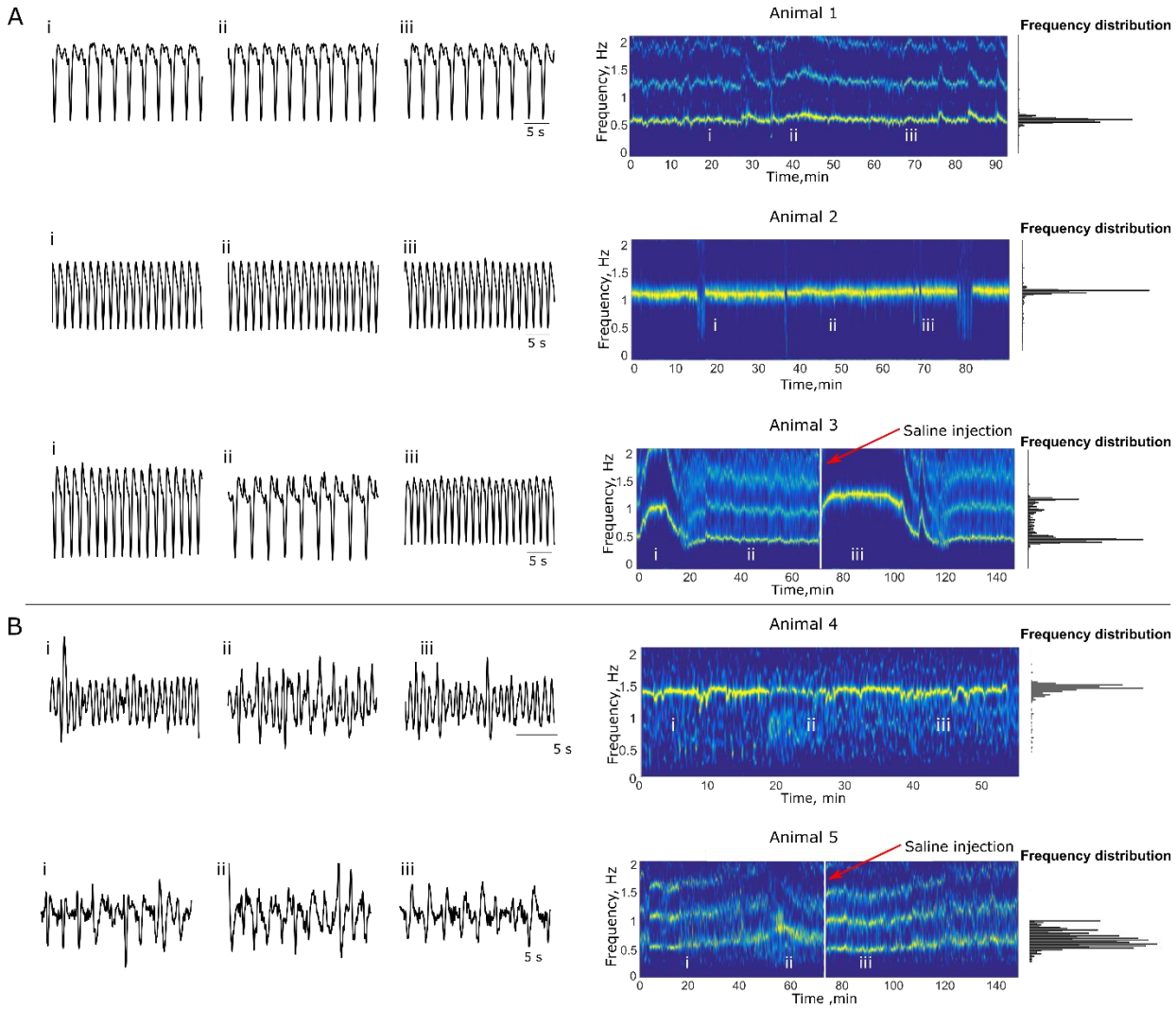

306
307 **Figure 2. Variability of heart and pyloric rhythm frequency at baseline conditions.**
308 **A)** Examples of cardiac rhythm recordings from three animals at different times during baseline
309 conditions (left) with their spectrograms (right). Roman numerals mark where 30-second raw
310 traces were taken from in the longer baseline frequency data (spectrograms). Animals 1 and 2
311 have stable low and high frequency cardiac rhythms respectively. The heart frequency of animal
312 3 switches between low and high frequency states spontaneously during baseline and after the
313 saline injection (indicated by vertical white line). **B)** Examples of pyloric rhythm recordings
314 from two animals during baseline conditions (left) with their spectrograms (right). Animal 4 has
315 a stable high frequency pyloric rhythm. Animal 5 has a more variable pyloric rhythm. The

316 pyloric rhythm frequency decreases after the saline injection (indicated by vertical white line).
317 Note that the waveforms of the pyloric rhythms are more complex than the waveforms of the
318 heart rhythm due to the complex movement patterns of the pyloric muscles.

319 Figure 3 summarizes pooled frequency data for the heart from 49 animals and
320 the pylorus from 29 animals. In all cases, the data came from stretches of recordings in
321 excess of 30 minutes. All of the pyloric rhythm data came from animals that were also
322 used for heart measurements. The histogram in Figure 3A shows an apparent
323 multimodal distribution of heart frequencies (Hartigan's dip test, dip=0.067, p =
324 0.029). Heart rhythm frequencies ranged between 0.4 Hz and 2.4 Hz (Fig. 3A). No
325 correlation was found between heart rhythm frequency and time of year of experiment
326 (p = 0.25, Pearson's correlation coefficient). Additionally, no correlation was found
327 between average heart rhythm frequency and weight of crab (p = 0.37, Pearson's
328 correlation coefficient).

329 Figure 3B shows a more normal distribution of the pyloric rhythm frequencies.
330 The spread in pyloric rhythm frequencies was much smaller than in heart frequencies,
331 ranging from 0.2 Hz to 1.6 Hz. In Figure 3C, we plotted the frequency of the pyloric
332 rhythm as a function of the heart rhythm for the 29 animals for which we had
333 measurements of both. Note that more than half of the points are not found close to the
334 identity line, suggesting that the pyloric and heart recordings are picking up rhythms in
335 the same general frequency range, but are not identical.

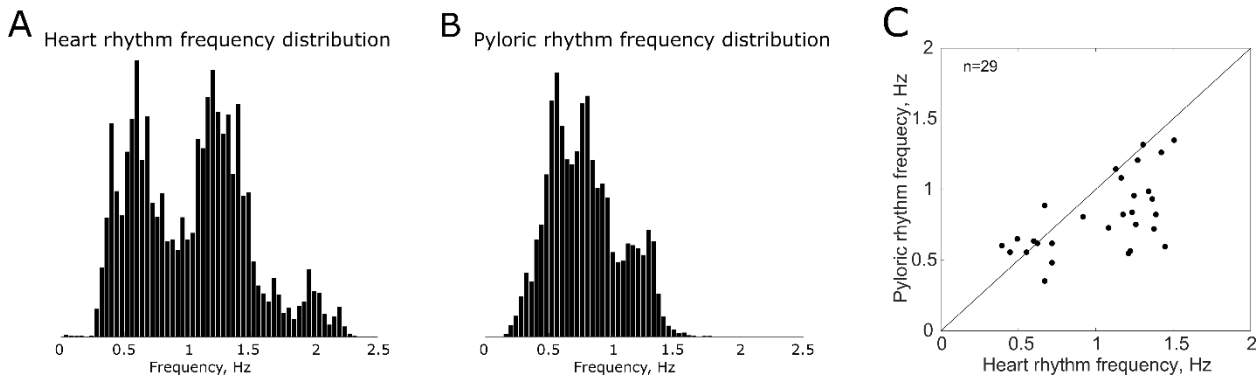

Figure 3. Frequency distributions of the heart and pyloric rhythms. A) The sum of normalized frequency distributions of heart rhythms of 49 animals at baseline conditions is multimodal. **B)** Sum of normalized frequency distributions of pyloric rhythms of 29 animals at baseline conditions. The spread in frequencies of the pyloric rhythms is smaller than of heart rhythms. **C)** Plot of baseline heart rhythm frequency versus pyloric rhythm frequency for each animal for which both were recorded. The pyloric frequency on average is lower than the heart rhythm frequency.

<u>Inhibitory bouts</u>

Heart rhythms often displayed periods of bradycardia, during which the heart considerably slowed or halted for a significant period (Fig. 4). We defined these periods as inhibitory bouts using a hidden Markov model (procedure described in the methods section). Periods of bradycardia were marked by a decrease in both amplitude and frequency (Fig. 4) of heart rhythm PPG recordings by at least 33% that lasted at least 10 seconds. An example of a 24 hr recording with multiple inhibitory bouts can be seen in Figure 4A. Termination of inhibitory bouts was associated with a return of amplitude and frequency. A temporary increase in amplitude of the heart signal could sometimes be observed immediately following the inhibitory bout (Fig A inset). Inhibitory bouts were seen in 20/49 animals of the population tested (41%). In most cases, when

inhibitory bouts were seen, they occurred repeatedly over extended periods of time, such as seen in the 24 hr recordings shown in Figure 4. Bout durations and frequency were variable both across and between animals (Fig. 4B). The occurrence of inhibitory bouts was not significantly correlated with the time of year (p = 0.79, Pearson's correlation coefficient) or weight of animal (p = 0.41, Pearson's correlation coefficient).

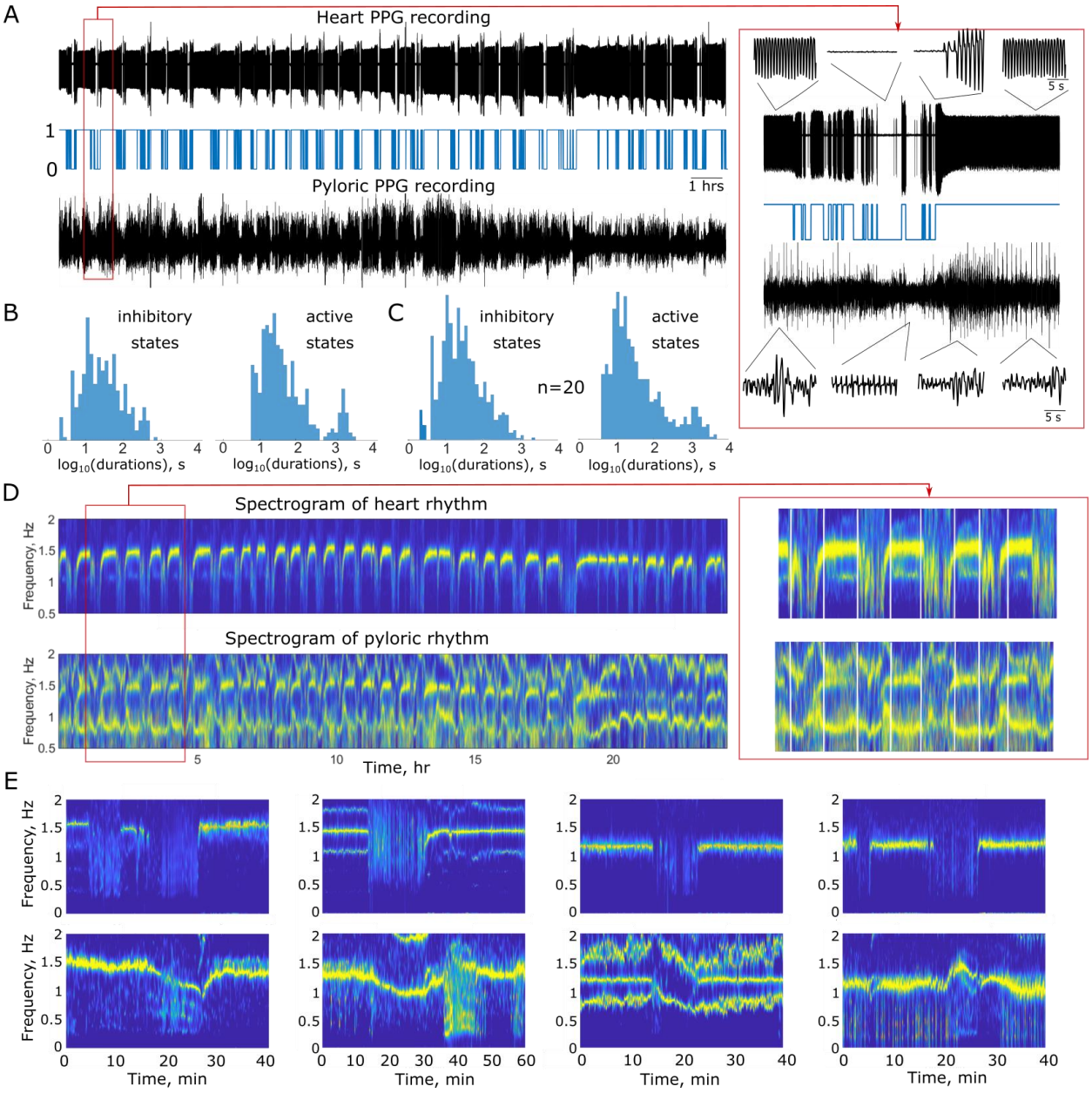

361 **Figure 4. The heart rhythm exhibits inhibitory bouts that influence the pyloric**
362 **rhythm**. **A)** Top panel, example of a 24 hour recording of the heart rhythm showing inhibitory
363 bouts throughout the recording session. Middle panel shows states identified from the heart
364 rhythm trace using hidden Markov model. State 1 corresponds to an active state and state 0
365 corresponds to an inhibitory bout. Bottom panel, simultaneously recorded pyloric rhythm.
366 Expanded traces during single inhibitory bout are shown in the red box. **B)** Distribution of
367 durations of active and inhibitory states of heart rhythm shown in A. **C)** Cumulative distribution
368 of durations of active and inhibitory states of heart activity of 20 animals. Heart rhythms of 20
369 out of 49 animals displayed inhibitory bouts with a mean duration of 30 s. Active state durations
370 display bimodal distribution. **D)** Top panel shows spectrogram of the heart rhythm shown in A.
371 The heart rhythm frequency in between the inhibitory bouts is maintained relatively constant at
372 1.5 Hz. Bottom panel shows spectrogram of the pyloric rhythm shown in **A**. The pyloric rhythm
373 decreases in frequency during the heart inhibitory bouts followed by the increase in frequency at
374 the end of the bouts. Zoomed in portion of the spectrogram is shown in the red box. **E)** More
375 examples of the frequency changes of the pyloric rhythm during and following the heart
376 inhibitory bouts from four different animals. Top panels are the spectrograms of heart activity
377 and bottom panels are the spectrograms of the pyloric activity. These data feature interaction
378 between the cardiac and the pyloric activity on the time scale of minutes.

379 Long periods of bradycardia affected the frequency and amplitude of pyloric
380 rhythm. Simultaneously recorded pyloric and heart signals in long-term experiments
381 show that the amplitude of the pyloric signal decreases during the inhibitory bout of the
382 heart (Fig 4A). Spectral analysis revealed that the frequency of the pyloric rhythm
383 modestly decreases during the heart inhibitory bouts (Fig. 4 C). However, there is
384 considerable variability in the changes in frequency of pyloric rhythm, as can be seen
385 from the spectrograms calculated during single inhibitory heart bout in 4 animals (Fig 4

386 D). For example, the experiments shown in the first panel illustrates an example when
387 the pyloric rhythm was reliably moving with a frequency of 1.5 Hz while the heart was
388 beating at 1.6 Hz. In this animal when the heart temporarily stopped, the pyloric rhythm
389 slowed to 0.9 Hz. The second example also shows a strong decrease in pyloric frequency
390 during the heart inhibitory bout. The third example showed a transient increase
391 followed by a decrease, while the fourth example showed a slight increase in frequency.

392 Relationships between the heart and pyloric rhythms. Although it is clear that
393 the pyloric rhythm and heart rhythms are often at different frequencies, and the pyloric
394 rhythm continues during the inhibitory bouts, spectrograms of the pyloric rhythm
395 frequently reveal a band at the heart frequency. This is very clearly illustrated in the
396 third example in Fig. 4D, where the heart rhythm is seen as a tight band at about 1.2 Hz.
397 That same band is seen below in the pyloric rhythm traces. When the heart stops, the
398 heart band disappears from both recordings.

399 To look at the potential influence of the heart rhythm on the pyloric rhythm, we
400 calculated the time-frequency coherence between simultaneously recorded heart and
401 pyloric rhythms in 2-minute bins moved in 5 second steps. In 70% of the animals, the
402 heart and pyloric rhythms were significantly coherent at the frequency of the heart more
403 than 50% of the time during the baseline period. Because the pyloric frequency often
404 changes when the heart stops, this suggests that some kind of biomechanical coupling or
405 common drive is influencing the two structures. Figure 5 A illustrates an example of
406 such coupling in an individual animal. The coherence peaks at 1.1 Hz frequency (Fig. 5
407 A), which is the frequency of heart oscillations shown in the spectrogram of the heart
408 signal (Fig 5A). The spectrogram of the pyloric rhythm has two frequency bands: one at

409 the frequency of approximately 0.5 Hz, which is intrinsic frequency of the pyloric
410 oscillations, and another on the heart rhythm frequency. By calculating the phase at the
411 frequency of peak coherence we determined that the pyloric rhythm is shifted by 190
412 degrees relative to the heart rhythm in this animal. This can also be seen from the cross-
413 correlation function, which has a minimum at 0.075 s lag. We also calculated auto-
414 correlations for the heart and pyloric rhythms. The pyloric rhythm has a more complex
415 auto-correlation function than the heart rhythm featuring two peaks, one peak on the
416 lag corresponding to the period of the heart oscillations and another peak on the period
417 of intrinsic pyloric oscillations. Figure 5 B illustrates one of the few examples when the
418 heart and pyloric rhythms were not coherent. The cross-correlation function of the two
419 rhythms in this example is flat. Overall, 28 out of 40 animals had coherent rhythms with
420 a magnitude of coherence more than 0.6 and phase differences between minus and plus
421 45 degrees (Fig. 5 C). There was no dependence of the percent of time the rhythms were
422 significantly coherent on the amplitude and frequency of the heart signal (Fig. 5C).

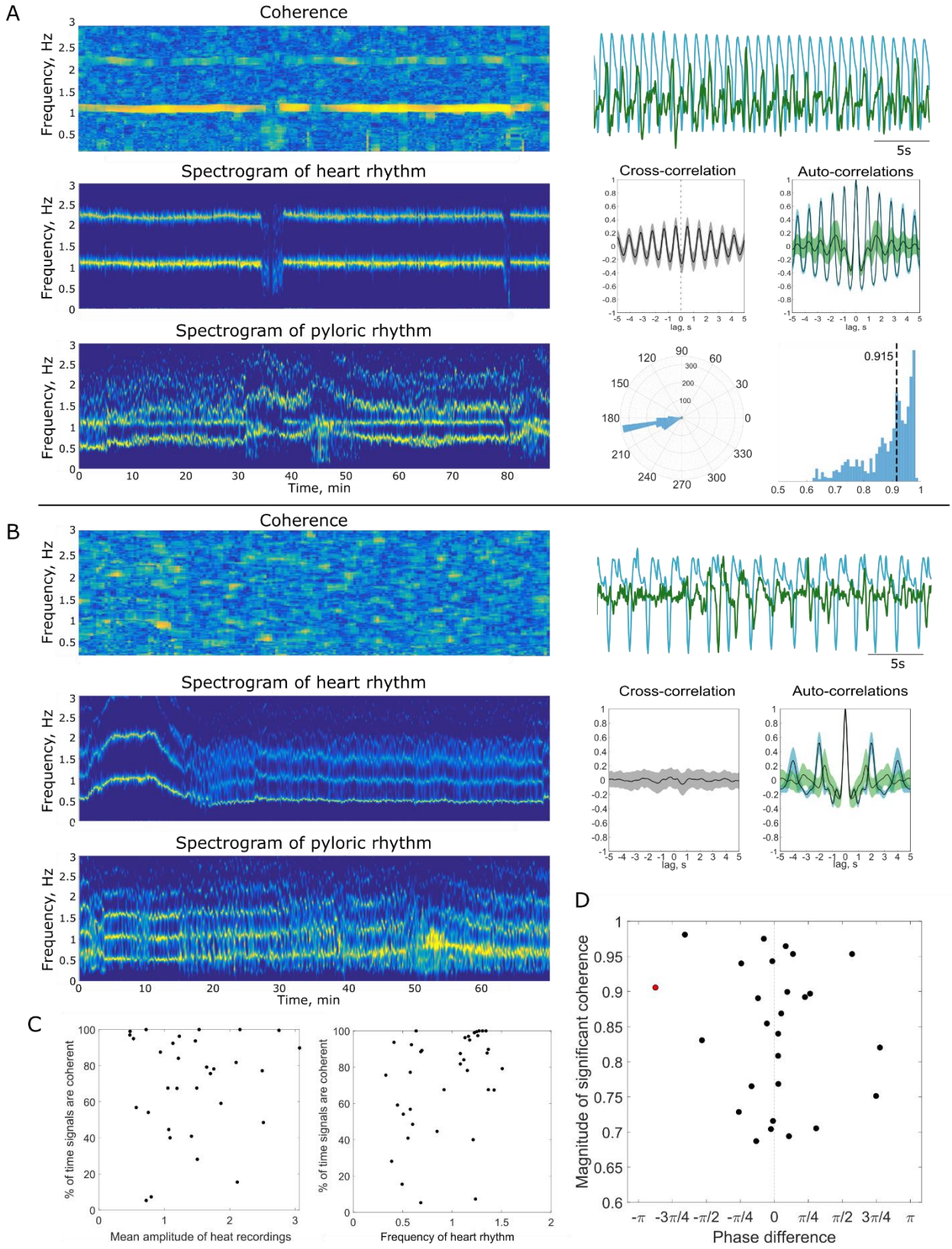
A
Coherence
Frequency, Hz
Spectrogram of heart rhythm
Spectrogram of pyloric rhythm
Time, min
5s
Cross-correlation
Auto-correlations
lag, s
0.915
B
C
% of time signals are coherent
Mean amplitude of heat recordings
Frequency of heart rhythm
D
Magnitude of significant coherence
Phase difference

423

Figure 5. Pyloric and heart rhythms are coherent at the frequency of the heart rhythm in the majority of animals. A) An example of high coherence between heart and pyloric rhythms from an individual animal. Top panel shows time-frequency coherence of the heart and pyloric rhythms at baseline. Middle panels show spectrograms of the heart and pyloric rhythms at baseline. Traces on the right show heart rhythm (blue) and pyloric rhythm (green), simultaneously recorded at baseline conditions. Data shown here are 30s segments of the full data range for which spectra and coherence were calculated. Below the traces, heart-pyloric cross-correlation (gray) and autocorrelation functions of heart (blue) and pyloric (green) rhythms are shown. The panel below shows the distribution of phase differences between the heart and pyloric rhythms calculated at 2 minute windows, moved in 10 s steps. The mean phase shift in this dataset is 190 degrees. Last panel, the distribution of magnitudes of peak coherence calculated at 2 minute windows, moved in 10 s steps. Median magnitude of peak coherence is 0.915. **B)** Example of the absence of coherence between the heart and pyloric rhythms from an individual animal. Top panel shows time-frequency coherence of heart and pyloric rhythms at baseline. Middle panels show spectrograms of heart and pyloric rhythms at baseline. Traces on the right are heart rhythm (blue) and simultaneously recorded pyloric rhythm (green) recorded at baseline. Data shown here are 30 s segments of the full data range for which spectra and coherence were calculated. Below the traces heart-pyloric cross-correlation (gray) and autocorrelation functions of heart (blue) and pyloric (green) rhythms are shown. **C)** Coherence statistics from all animals with simultaneous recordings of heart and pyloric rhythms (n=40). The left panel shows the percentage of time pyloric and heart rhythms are significantly coherent at baseline versus the amplitude of the recorded heart signal. The middle panel shows percentage of time pyloric and heart rhythms are significantly coherent at baseline versus the frequency of heart rhythm. **D)** Scatter plot showing median magnitudes of peak coherence versus median phase difference between heart and pyloric rhythms. The pyloric and heart rhythms were significantly coherent >50% of time in 70% of animals.

450 Effects of temperature on heart and pyloric rhythms. We tested the effects of
451 increasing temperature on the heart movements of twelve animals and on pyloric
452 movements in nine animals (Fig. 6). Figure 6A shows raw data from a typical
453 experiment showing heart and pyloric movements during a temperature ramp from 11°C
454 to 28°C and then back to 11°C. Figure 6B shows plots of the heart and pyloric rhythm
455 frequency for three animals as a function of the temperature. Frequency was calculated
456 for both heart and pyloric rhythms as the frequency at the peak of the power spectrum
457 density of the rhythms in each sliding window. In all the heart movement recordings,
458 the frequency increased with increasing temperature until crashes of the heart rhythm
459 occurred. Rhythm crashes were characterized by the occurrence of low frequency and
460 irregular patterns of activity. Crash of the heart rhythm is followed by the recovery of
461 activity as the temperature decreases. Note that despite the common pattern in which
462 hearts of different animals respond to changes to the temperature, there is across
463 animal variability in the heart rhythm activity in response to almost identical
464 temperature ramps. Particularly, maximal frequencies, critical temperatures and
465 recovery patterns are different in different animals (Fig. 6B). In the pyloric recordings,
466 waveforms changed in overall shape, often exhibiting peaks followed by long plateaued
467 waveforms. Similar to the heart activity, the frequency of the pyloric rhythm also
468 increased with increasing temperature, again characterized by irregular periods of
469 "crashed" activity at high temperatures.

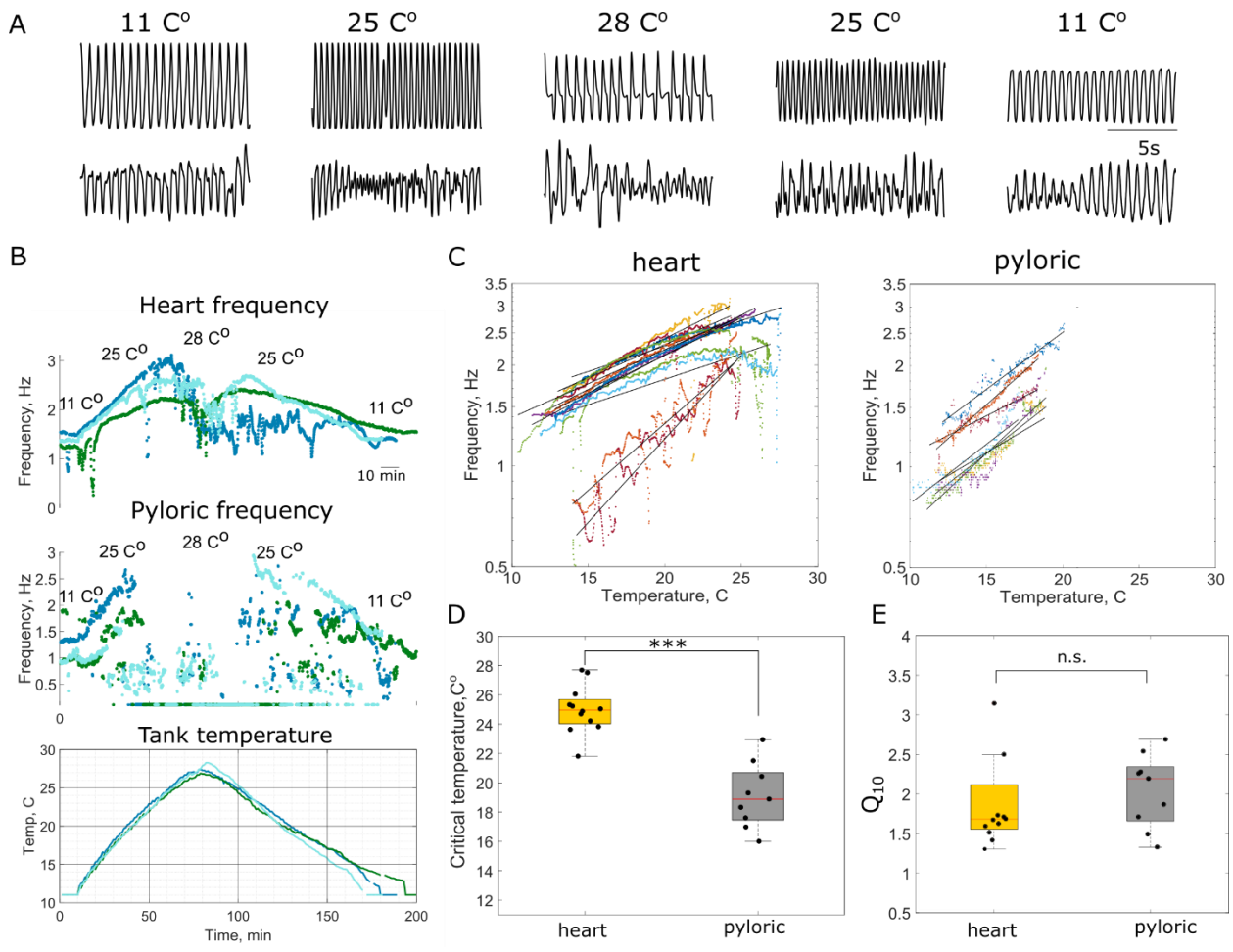

Figure 6. The pyloric rhythm is more sensitive to increases in temperature than is the heart rhythm. A) Raw traces of heart and pyloric muscle activity at baseline (11°C), during increasing (25°C), critical (28°C) and decreasing portions (25°C) of the temperature ramp. **B)** Top trace shows the change in frequency of heart rhythms of three animals in response to almost identical temperature ramps shown in the bottom panel. Middle trace shows the change in frequency of simultaneously recorded pyloric rhythm in response to the temperature ramp. The pyloric rhythm is less robust to the increases in temperature than the heart rhythm and crashes at a much lower temperature. "Crash" is evident by significant decrease in frequency and amplitude of the pyloric rhythm. **C)** Frequencies of the heart and pyloric rhythms during increasing portion of temperature ramps plotted as a function of a temperature in a logarithmic scale, each color corresponds to an individual animal. A line was fit to data points

482 for each animal's heart frequencies to estimate Q_{10}s. **D)** Critical temperature of the heart
483 rhythm is significantly higher than of the pyloric rhythm *(*mean heart critical temperature
484 $T_{Hr_critical} = 25 \pm 1.62\,C^{\circ}$, mean pyloric critical temperature $T_{P_critical} = 19.1 \pm 2.76$, *one-way*
485 *ANOVA, p=0.0005, F(1,19)=21.07).* **E)** Q_{10}s of heart and pyloric frequencies are not significantly
486 different (*mean Q10 of heart frequency is* 2.007 ± 0.854*, mean Q10 of pyloric frequency is*
487 2.04 ± 0.467*, one-way ANOVA, p=0.9155, F(1,19)=0.01*).

488 Frequencies of the heart and pyloric rhythms are plotted as a function of
489 temperature in a logarithmic scale in Figure 6C. Linear models were fitted to the data
490 points for each animal to estimate heart and pyloric frequency Q_{10}s. The pyloric
491 rhythms consistently crashed at lower temperatures than the heart rhythm in the same
492 animal. The critical temperature was defined as the temperature at which cardiac or
493 pyloric stability and regularity was lost, with a subsequent drop in contraction frequency
494 to near baseline values. Critical temperatures of the heart muscle movements were
495 collected for all twelve animals and for the pyloric muscle movements for nine animals
496 (Fig. 6D). The mean heart critical temperature was 25.0°C (s.d. = 1.62) and the mean
497 pyloric critical temperature was 19.1°C (s.d. = 2.76) (Fig. 6D). The critical temperatures
498 of the heart and pyloric muscle movements were significantly different (*one-way*
499 *ANOVA, p=0.0005, F(1,19)=21.07*).

500 Q_{10}, a measurement of the rate of change of a biological process in response to a
501 change in temperature, was calculated for both the heart and pyloric rhythm for each
502 animal tested (Fig. 6E). The frequency of the heart and pyloric rhythms was plotted as a
503 function of environmental temperature in a logarithmic scale and linear regression
504 model was fitted into data points (Fig. 6E). Coefficients of determinations (R^2) for each

505 fit are shown in table in methods section. Q_{10}s were calculated as slopes of linear
506 models. Q_{10}s for heart rhythms, ranged from 1.3 to 4.2 with a mean of 2.007 (s.d. =
507 0.854). Pyloric rhythm Q_{10}s ranged from 1.33 to 2.7 with a mean of 2.04 (s.d. = 0.47).
508 The Q_{10}s of the heart and pyloric rhythms were not significantly different as determined
509 by *one-way ANOVA* ($p=0.127$, $F(1,19)=2.54$).

510 Finally, we calculated the coherence between the heart and pyloric rhythms
511 during the temperature ramps to determine whether temperature perturbation affects
512 the relationship between signals. An example time-frequency coherence from an
513 individual animal is shown in Figure 7A. The coherence peaks at the frequency of heart
514 oscillations at baseline as well as during the temperature ramps. Examples of coherence
515 and phase differences calculated at different stages of the experiment (baseline, rising
516 phase of temperature ramp, and decreasing phase of temperature ramp) show that the
517 amplitude of the coherence remains high throughout the whole experiment and the
518 temperature perturbation does not affect the phase relationship between rhythms. In
519 this example the rhythms oscillate in phase (phase difference at the frequency of
520 maximal coherence is shown by arrows in Figure 7C). Peak coherence at baseline and
521 during the rising phase of the temperature ramp as well as the percent of time the
522 rhythms were coherent and their phase difference were calculated for all nine
523 temperature experiments with simultaneously recorded heart and pyloric rhythms (Fig
524 7D). Coherence between signals was calculated up to the point of the pyloric rhythm
525 crash. There were no statistically significant differences between mean peak coherences
526 at baseline and during the temperature ramps as determined by one-way ANOVA (
527 $p=0.806$, $F(1,32)=0.06$). Similarly, there were no statistically significant differences

between mean phase differences at baseline and during the temperature ramps as determined by one-way ANOVA (*p=0.759, F(1,32)=0.1*). Finally, the rhythms were coherent approximately the same amount of time at baseline and during the rising phase of the temperature ramp (one-way ANOVA, *p=0.354, F(1,16)=0.91*). In the majority of the datasets, the rhythms were coherent 100% of the time. Together, these data suggest that rhythms that are coherent at baseline remain coherent during the increase of environmental temperature without a significant change in phase relationship.

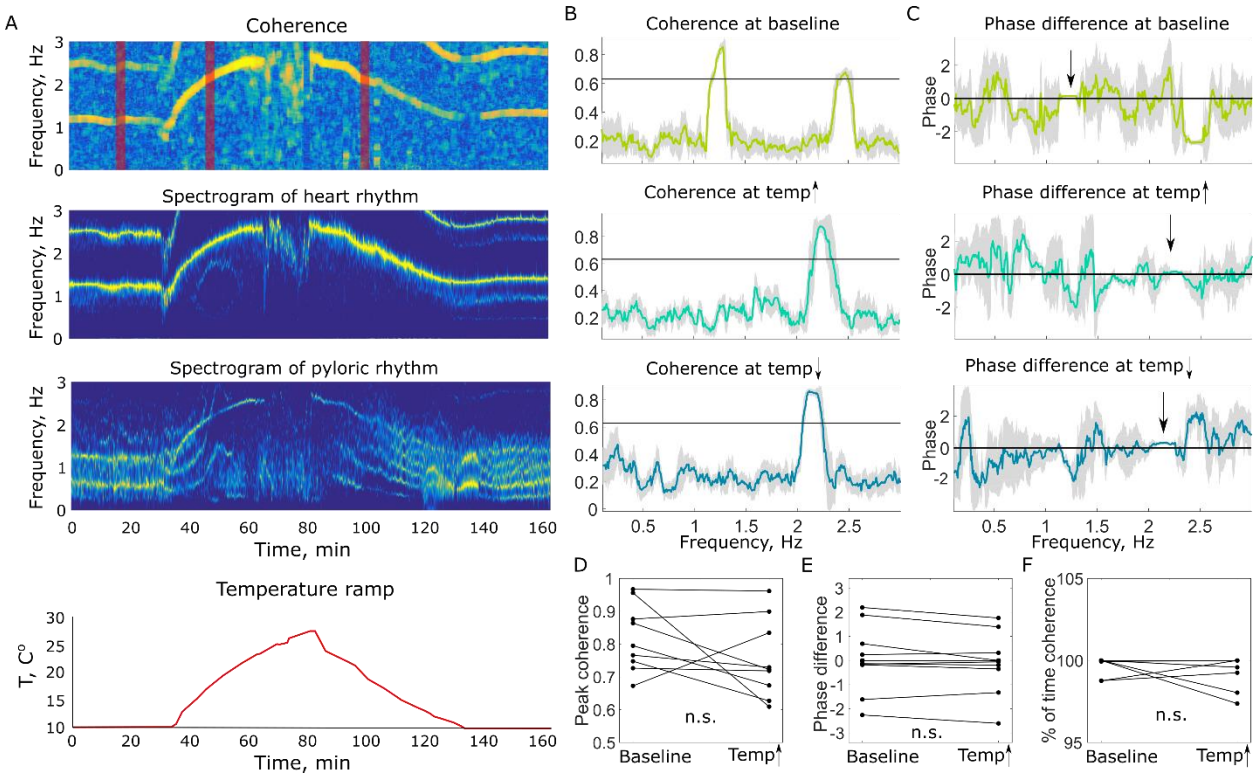

Figure 7. Coherent heart and pyloric rhythms remain coherent during the temperature ramp without change in phase relationship. A) An example of coherence between heart and pyloric rhythms and spectrograms of the rhythms at baseline and during temperature ramp from an individual animal. Bottom panel shows temperature in the tank

during the experiment. **B)** Examples of coherence at baseline, during rising and decaying phases of temperature ramps. Horizontal black line shows theoretical significance level. The times at which example coherences were taken are shown by the red bars in part A. Rhythms are coherent throughout the whole experiment at frequency of heart rhythm. **C)** Phase difference of the rhythms in A at baseline, during rising and decaying phases of temperature ramps. Phase difference between heart and pyloric rhythm remains constant throughout the whole experiments. **D)** Peak coherence between heart and pyloric rhythms from all temperature experiments ($n=9$) at baseline and during rising phase of temperature ramp. Coherence during temperature ramp was calculated up to the critical temperature of the pyloric rhythm. There were no statistically significant differences between mean peak coherences at baseline and during the temperature ramp as determined by one-way ANOVA, $p=0.806$, $F(1,32)=0.06$. **E)** Phase difference between heart and pyloric rhythms were calculated for all temperature experiments ($n=9$). There were no statistically significant differences between mean phase differences at baseline and during temperature ramp as determined by one-way ANOVA, $p=0.759$, $F(1,32)=0.1$. **F)** Percent of time heart and pyloric rhythms were coherent. There were no statistically significant differences between mean percent of time rhythms were coherent at baseline and during temperature ramp as determined by one-way ANOVA, $p=0.354$, $F(1,16)=0.91$. In majority of the datasets rhythms were coherent %100 of time.

559 **Discussion**

560 It is always interesting to determine the extent to which different body rhythms
561 are correlated in their activity. This is especially interesting with respect to the heart
562 and stomach rhythms in crustaceans because the stomatogastric ganglion is situated
563 just anterior to the heart in the dorsal artery, where it is directly perfused by
564 hemolymph containing hormones released into the circulatory system. To the best of
565 our knowledge, ours is the first study to record simultaneously the heart and stomach's
566 pyloric rhythms both under control conditions and in response to temperature changes.

567 <u>Baseline Functioning of the Heart Rhythm</u>

568 The crustacean heart is neurogenic, and therefore the activity of the cardiac
569 ganglion directly regulates the heart beat frequency. The CG must be able to produce
570 activity regularly and across a wide range of perturbations. It must be modifiable to
571 adjust to the animal's metabolic needs (Dickinson et al., 2016b; Dickinson et al., 2015b;
572 Robertson and Money, 2012) and reliable enough to ensure that the heart continues to
573 pump hemolymph at all times. Both frequency and contraction amplitude, two factors
574 which must be regulated to ensure the animals' success, are expressions of the activity of
575 the CG, specifically its interburst interval, rate, and firing patterns.

576 We captured heart activity using PPG recording techniques while limiting the
577 invasiveness and stress placed on the animal. PPG recordings of the heart musculature
578 were reliable over time and showed differences in frequency of heart beats within the
579 population (Fig. 2). In the majority of experiments, an animal's baseline heart rate was
580 relatively stable (Fig. 2), but in some animal's frequency switches were spontaneously
581 seen (Fig. 2A, animal 3). During baseline recordings, animals were not subjected to

582 changes in temperature, light, salinity, stress or environmental factors that could
583 interact with the metabolic needs of the animal or the functions of the CG. During this
584 time, the firing of the CG, and therefore the activity of the heart, would not be expected
585 to appreciably change. Nonetheless, the heart rate of resting animals falls into a
586 multimodal distribution. These data suggest that heart activity, and therefore activity of
587 the CG, falls into states of higher or lower activity. These states may be a consequence of
588 variable metabolic needs of the animal during the time of recording, such as digestion,
589 movement, or excretion. The CG may therefore have mechanisms for switching between
590 high and low activity states through neuromodulation or extrinsic neural input.
591 Alternatively, the high and low activity states may reflect circatidal (rhythms that are
592 governed by the tide) (Chabot and Watson, 2010a) or circadian rhythms the animal
593 experiences (Chabot and Watson, 2010b; De La Iglesia and Hsu Y., 2010).

594 Several animals displayed heart inhibitory bouts, periods of bradycardia during
595 which the heart slowed or completely stopped for a minimum of 10 seconds. These
596 inhibitory bouts persisted throughout an entire experiment, and likely last through long
597 periods in an animal's life. Within an animal, inhibitory bouts persist for extended
598 periods of time during a long recording session (Fig. 4B). Inhibitory bouts have
599 previously been observed as linked to times of gill ventilation during reversal of
600 pumping of the scaphognathite (McMahon, 1999). This is likely due to overflow of ocean
601 water, and therefore oxygen, in the gills, causing the organism's heart to stop for a
602 significant period. It is interesting, however, that this occurs in only about 41% of
603 animals tested. This implies a mechanism affecting both the heart and the gills that
604 influences the overall levels of dissolved O_2 within the animal.

605 Baseline Function of the Pyloric Rhythm

606 The STG maintains its triphasic rhythm to control the movement of the muscles,
607 and is robust to several global perturbations, including temperature (Soofi et al., 2014;
608 Tang et al., 2010; Tang et al., 2012) and pH (Haley, Hampton and Marder, 2018).
609 Previous work has shown the importance of animal-to-animal variability in responses to
610 such perturbations (Hamood et al., 2015; Hamood and Marder, 2014; Hamood and
611 Marder, 2015). Interestingly, there are differential sensitivities of the responses of
612 isolated STGs and cardiac ganglia to pH, again with the cardiac ganglion being more
613 robust. However, no one has previously compared the *in vivo* responses of the heart
614 and pylorus to any perturbation.

615 In the experiments presented here, PPG sensors recording the muscle movement
616 of the pylorus were placed on the carapace above the dorsal dilator muscle. While heart
617 rhythm waveforms were relatively simple, with one maximum and minimum, pyloric
618 rhythm waveforms were more complex (Fig. 2B). The complexity of the PPG waveform
619 is likely due to the positioning of the muscles being recorded and their movements in
620 relation to the PPG sensor. *In vivo,* the pyloric rhythm frequency drifts more than that
621 of the heart rhythm frequency over a baseline period. Across the population of tested
622 and analyzed animals, the pyloric rhythm had a more normal distribution, unlike that of
623 the heart rhythm (Fig. 3).

624 Comparison of the Heart and Pyloric Rhythms

625 While the generation and movement of the heart and pylorus have been
626 extensively studied separately in the past, here we examined the potential interactions
627 between these two central pattern generated movements. To determine how these two

628 essential rhythms may interact in a single animal, we calculated time-frequency
629 coherence between the rhythms of animals in controlled environments. In a majority of
630 animals, the heart and pyloric rhythms were coherent at the frequency of the heart
631 rhythm (Fig. 5A). We know that this coherence is not simple cross-talk between the
632 sensors themselves, as the pyloric rhythm continues when the heart stops (Fig. 4C,D),
633 and because there are numerous instances when the two rhythms are quite different.
634 We suspect that the coherence between the two rhythms is a bio-mechanical coupling
635 between the heart and the stomach, which are situated close to each other under the
636 dorsal carapace. Moreover, the dorsal artery runs between the paired dorsal dilator
637 muscles (the source of the pyloric signal) and the PPG sensor placed above the posterior
638 part of the stomach may pick up pulsations of the artery that occur with each heartbeat.

639 Temperature as a Perturbation to Expose the Mutual Changes in the Heart and Pyloric
640 Rhythms

641 Previous work on temperature has shown that both the heart and pyloric rhythms
642 increase in frequency with increases in temperature (Marder et al., 2015; Soofi et al.,
643 2014; Tang et al., 2010; Worden et al., 2006). Both rhythms are also known to crash
644 beyond critical temperatures, at which point the muscles no longer move in canonical
645 patterns (Soofi et al., 2014; Tang et al., 2012), and it is likely that the muscles
646 themselves cannot contract correctly at high temperatures. In intertidal worms, the
647 heart critical temperature likely corresponds with the onset of anaerobic metabolism,
648 due to a mismatch between the animal's oxygen needs and the supply being delivered to
649 the heart (Zielinski and Portner, 1996).

650 In the data presented here, it is clear that temperature affects both rhythms and
651 increases their overall frequency, with similar Q_{10}s (Fig. 6E). This indicates that
652 increases in temperature cause similar changes in the two frequencies, until a crash
653 point occurs. Interestingly, the heart is more robust to extreme temperature changes
654 than the pyloric rhythm.

655 Crabs can live for days and weeks without eating, but presumably cannot survive
656 for extended periods of time without hemolymph oxygenation and circulation. From
657 this perspective, it is easy to justify the fact that the critical temperature for the heart
658 rhythm is higher than that for the pyloric rhythm. The additional 4-5°C might make a
659 big difference for an animal caught in shallow water during the summer, and give it time
660 to find its way to more hospitable environments. Interestingly, the mean critical
661 temperatures are within the range that *C. borealis* might experience during a New
662 England summer in shallow water or intertidal adventures. The animal-to-animal
663 variability in these critical temperatures may be important signatures that explain the
664 survival of some animals during summer heat.

665

666

Acknowledgements

We thank Dr. Markus Frederich for an introduction into the use of PPG system, and Jessica Haley for assistance in early data analysis. Data in this paper were first presented for partial fulfilment of requirements for BS/MS program (DK) at Brandeis University.

Competing Interests

The authors declare no competing or financial interests.

Funding

This work was supported by National Institutes of Health R35 NS 097343 to E.M.

686 # References

687 **Alexandrowicz, J. S. and Carlisle, D. B.** (1953). Some experiments on the function of the
688 pericardial organs in Crustacea. *J. Mar. Biol. Assoc. U.K.* **32**, 175-192.
689 **Bilmes, J. A.** (1998). A Gentle Tutorial of the EM Algorithm and its Application to Parameter
690 Estimation for Gaussian Mixture and Hidden Markov Models. . In *International Computer Science*
691 *Institute*, pp. 7-13. Berkeley, CA.
692 **Burg, J. P.** (1967). Maximum entropy spectral analysis. In *Proc. 37th Meeting Society of*
693 *Exploration Geophysicist*. Oklahoma City, OK.
694 **Buttkus, B.** (2000). Spectral Analysis and Filter Theory. Berlin: Springer.
695 **Camacho, J., Qadri, S. A., Wang, H. and Worden, M. K.** (2006). Temperature acclimation alters
696 cardiac performance in the lobster *Homarus americanus*. *J Comp Physiol A Neuroethol Sens Neural*
697 *Behav Physiol* **192**, 1327-34.
698 **Caplan, J. S., Williams, A. H. and Marder, E.** (2014). Many parameter sets in a
699 multicompartment model oscillator are robust to temperature perturbations. *J Neurosci* **34**, 4963-75.
700 **Chabot, C. C. and Watson, W. H.** (2010a). Circatidal rhythms of locomotion in the American
701 horseshoe crab *Limulus polyphemus:* Underlying mechanisms and cues that influence them. *Current*
702 *Zoology* **56**, 499-517.
703 **Chabot, C. C. and Watson, W. H.** (2010b). Horseshoe crab behavior: Patterns and processes.
704 *Current Zoology* **56**, I-Iii.
705 **Chen, R., Jiang, X., Conaway, M. C., Mohtashemi, I., Hui, L., Viner, R. and Li, L.** (2010). Mass
706 spectral analysis of neuropeptide expression and distribution in the nervous system of the lobster
707 *Homarus americanus*. *J Proteome Res* **9**, 818-32.
708 **Christie, A. E., Cashman, C. R., Stevens, J. S., Smith, C. M., Beale, K. M., Stemmler, E. A.,**
709 **Greenwood, S. J., Towle, D. W. and Dickinson, P. S.** (2008). Identification and cardiotropic actions of
710 brain/gut-derived tachykinin-related peptides (TRPs) from the American lobster Homarus americanus.
711 *Peptides* **29**, 1909-18.
712 **Christie, A. E., Skiebe, P. and Marder, E.** (1995). Matrix of neuromodulators in neurosecretory
713 structures of the crab Cancer borealis. *J Exp Biol* **198**, 2431-9.
714 **Clemens, S., Combes, D., Meyrand, P. and Simmers, J.** (1998a). Long-term expression of two
715 interacting motor pattern-generating networks in the stomatogastric system of freely behaving lobster.
716 *J. Neurophysiol.* **79**, 1396-408.
717 **Clemens, S., Massabuau, J.-C., Meyrand, P. and Simmers, J.** (1999). Changes in motor network
718 expression related to moulting behaviour in lobster: role of moult-induced deep hypoxia. *J. Exp. Biol.*
719 **202**, 817-827.
720 **Clemens, S., Massabuau, J. C., Legeay, A., Meyrand, P. and Simmers, J.** (1998b). *In vivo*
721 modulation of interacting central pattern generators in lobster stomatogastric ganglion: influence of
722 feeding and partial pressure of oxygen. *J. Neurosci.* **18**, 2788-99.
723 **Clemens, S., Massabuau, J. C., Meyrand, P. and Simmers, J.** (2001). A modulatory role for
724 oxygen in shaping rhythmic motor output patterns of neuronal networks. *Respir Physiol* **128**, 299-315.
725 **Clemens, S., Meyrand, P. and Simmers, J.** (1998c). Feeding-induced changes in temporal
726 patterning of muscle activity in the lobster stomatogastric system. *Neurosci. Lett.* **254**, 65-8.
727 **Cooke, I. M.** (2002). Reliable, responsive pacemaking and pattern generation with minimal cell
728 numbers: the crustacean cardiac ganglion. *Biol Bull* **202**, 108-36.
729 **Cruz-Bermudez, N. D. and Marder, E.** (2007). Multiple modulators act on the cardiac ganglion of
730 the crab, *Cancer borealis*. *J Exp Biol* **210**, 2873-84.

731 **De La Iglesia, H. O. and Hsu Y., W. A.** (2010). Biological clocks and rhythms in intertidal
732 crustaceans. . *Frontiers in Bioscience—Elite. 2010* **2**, 1394–1404.
733 **DeKeyser, S. S., Kutz-Naber, K. K., Schmidt, J. J., Barrett-Wilt, G. A. and Li, L.** (2007). Imaging
734 mass spectrometry of neuropeptides in decapod crustacean neuronal tissues. *J Proteome Res* **6**, 1782-
735 91.
736 **Depledge, M. H.** (1983). Photoplethysmography – A non-invasive technique for monitoring
737 heart beat and ventilation rate in Decapod Crustaceans. *Comp. Biochem Physiol* **77A**, 369-371.
738 **Dickinson, E. S., Johnson, A. S., Ellers, O. and Dickinson, P. S.** (2016a). Forces generated during
739 stretch in the heart of the lobster *Homarus americanus* are anisotropic and are altered by
740 neuromodulators. *J Exp Biol* **219**, 1187-202.
741 **Dickinson, P. S., Calkins, A. and Stevens, J. S.** (2015a). Related neuropeptides use different
742 balances of unitary mechanisms to modulate the cardiac neuromuscular system in the American lobster,
743 *Homarus americanus*. *J Neurophysiol* **113**, 856-70.
744 **Dickinson, P. S., Qu, X. and Stanhope, M. E.** (2016b). Neuropeptide modulation of pattern-
745 generating systems in crustaceans: comparative studies and approaches. *Curr Opin Neurobiol* **41**, 149-
746 157.
747 **Dickinson, P. S., Sreekrishnan, A., Kwiatkowski, M. A. and Christie, A. E.** (2015b). Distinct or
748 shared actions of peptide family isoforms: I. Peptide-specific actions of pyrokinins in the lobster cardiac
749 neuromuscular system. *J Exp Biol* **218**, 2892-904.
750 **Hamood, A. W., Haddad, S. A., Otopalik, A. G., Rosenbaum, P. and Marder, E.** (2015).
751 Quantitative reevaluation of the effects of short- and long-term removal of descending modulatory
752 inputs on the pyloric rhythm of the crab, *Cancer borealis*. *ENEURO* **2**, 0058-14.
753 **Hamood, A. W. and Marder, E.** (2014). Animal-to-Animal Variability in Neuromodulation and
754 Circuit Function. *Cold Spring Harb Symp Quant Biol* **79**, 21-8.
755 **Hamood, A. W. and Marder, E.** (2015). Consequences of acute and long-term removal of
756 neuromodulatory input on the episodic gastric rhythm of the crab *Cancer borealis*. *J Neurophysiol* **114**,
757 1677-92.
758 **Heinzel, H. G.** (1988). Gastric mill activity in the lobster. I. Spontaneous modes of chewing. *J.*
759 *Neurophysiol.* **59**, 528-550.
760 **Heinzel, H. G. and Selverston, A. I.** (1988). Gastric mill activity in the lobster. III. Effects of
761 proctolin on the isolated central pattern generator. *J. Neurophysiol.* **59**, 566-585.
762 **Hooper, S. L. and Marder, E.** (1987). Modulation of the lobster pyloric rhythm by the peptide
763 proctolin. *J. Neurosci.* **7**, 2097-2112.
764 **Hui, L., Xiang, F., Zhang, Y. and Li, L.** (2012). Mass spectrometric elucidation of the
765 neuropeptidome of a crustacean neuroendocrine organ. *Peptides* **36**, 230-9.
766 **Johnson, B. and Hooper, S.** (1992). Overview of the stomatogastric nervous system. In *Dynamic*
767 *Biological Networks*, eds. R. Harris-Warrick E. Marder A. Selverston and M. Moulins), pp. 1-30.
768 Cambridge, MA: MIT Press.
769 **Marder, E.** (2012). Neuromodulation of neuronal circuits: back to the future. *Neuron* **76**, 1-11.
770 **Marder, E. and Bucher, D.** (2007). Understanding circuit dynamics using the stomatogastric
771 nervous system of lobsters and crabs. *Annu Rev Physiol* **69**, 291-316.
772 **Marder, E., Haddad, S. A., Goeritz, M. L., Rosenbaum, P. and Kispersky, T.** (2015). How can
773 motor systems retain performance over a wide temperature range? Lessons from the crustacean
774 stomatogastric nervous system. *J Comp Physiol A Neuroethol Sens Neural Behav Physiol* **201**, 851-6.
775 **Maynard, D. M.** (1972). Simpler networks. *Ann. NY Acad. Sci.* **193**, 59-72.
776 **Maynard, D. M. and Dando, M. R.** (1974). The structure of the stomatogastric neuromuscular
777 system in *Callinectes sapidus*, *Homarus americanus* and *Panulirus argus* (decapoda crustacea). *Philos.*
778 *Trans. R. Soc. Lond. (Biol.)* **268**, 161-220.

McGaw, I. J. and McMahon, B. R. (1996). Cardiovascular responses resulting from variation in external salinity in the dungeness crab, Cancer magister. *Physiological Zoology* **69**, 1384-1401.

McMahon, B. R. (1995). The physiology of gas exchange, circulation, ion regulation and nitrogenous excretion: an integrative approach. In *Biology of the Lobster Homarus americanus*, (ed. J. R. Factor), pp. 497-517. San Diego: Academic Press.

McMahon, B. R. (1999). Intrinsic and extrinsic influences on cardiac rhythms in crustaceans. *Comparative Biochemistry and Physiology a-Molecular and Integrative Physiology* **124**, 539-547.

McMahon, B. R. (2001a). Control of cardiovascular function and its evolution in Crustacea. *J Exp Biol* **204**, 923-32.

McMahon, B. R. (2001b). Respiratory and circulatory compensation to hypoxia in crustaceans. *Respir Physiol* **128**, 349-64.

Mitra, P. P., Pesaran, B. and (1999). Analysis of dynamic brain imaging data. . *Biophys J.* **76**, 691-708.

Morris, L. G. and Hooper, S. L. (1997). Muscle response to changing neuronal input in the lobster (*Panulirus interruptus*) stomatogastric system: spike number-versus spike frequency-dependent domains. *J. Neurosci.* **17**, 5956-5971.

Morris, L. G. and Hooper, S. L. (1998). Muscle response to changing neuronal input in the lobster (*Panulirus interruptus*) stomatogastric system: slow muscle properties can transform rhythmic input into tonic output. *J. Neurosci.* **18**, 3433-3442.

Morris, L. G. and Hooper, S. L. (2001). Mechanisms Underlying Stabilization of Temporally Summated Muscle Contractions in the Lobster (*Panulirus*) Pyloric System. *J Neurophysiol* **85**, 254-268.

O'Leary, T. and Marder, E. (2016). Temperature-robust neural function from activity-dependent ion channel regulation. *Current Biology* **26**, 2935-2941.

Rabiner, L. R. (1989). A tutorial on hidden Markov models and selected applications in speech recognition. *Proceedings of the IEEE 77, 257–286* **77**, 257-286.

Rezer, E. and Moulins, M. (1983). Expression of the crustacean pyloric pattern generator in the intact animal. *J. Comp. Physiol. A* **153**, 17-28.

Rinberg, A., Taylor, A. L. and Marder, E. (2013). The effects of temperature on the stability of a neuronal oscillator. *PLoS Comput Biol* **9**, e1002857.

Robertson, R. M. and Money, T. G. (2012). Temperature and neuronal circuit function: compensation, tuning and tolerance. *Curr Opin Neurobiol* **22**, 724-34.

Soofi, W., Goeritz, M. L., Kispersky, T. J., Prinz, A. A., Marder, E. and Stein, W. (2014). Phase maintenance in a rhythmic motor pattern during temperature changes *in vivo*. *J Neurophysiol* **111**, 2603-2613.

Sullivan, R. E. and Miller, M. W. (1984). Dual effects of proctolin on the rhythmic burst activity of the cardiac ganglion. *J Neurobiol* **15**, 173-96.

Tang, L. S., Goeritz, M. L., Caplan, J. S., Taylor, A. L., Fisek, M. and Marder, E. (2010). Precise temperature compensation of phase in a rhythmic motor pattern. *PLoS Biol* **8**, e1000469.

Tang, L. S., Taylor, A. L., Rinberg, A. and Marder, E. (2012). Robustness of a rhythmic circuit to short- and long-term temperature changes. *J Neurosci* **32**, 10075-85.

Wilkens, J. L. and McMahon, B. R. (1994). Cardiac performance in semi-isolated heart of the crab Carcinus maenas. *Am J Physiol* **266**, R781-9.

Williams, A. H., Calkins, A., O'Leary, T., Symonds, R., Marder, E. and Dickinson, P. S. (2013). The neuromuscular transform of the lobster cardiac system explains the opposing effects of a neuromodulator on muscle output. *J Neurosci* **33**, 16565-75.

Worden, M. K., Clark, C. M., Conaway, M. and Qadri, S. A. (2006). Temperature dependence of cardiac performance in the lobster *Homarus americanus*. *J Exp Biol* **209**, 1024-34.

826 **Zielinski, S. and Portner, H. O.** (1996). Energy metabolism and ATP free-energy change of the
827 intertidal worm Sipunculus nudus below a critical temperature. *Journal of Comparative Physiology B-*
828 *Biochemical Systemic and Environmental Physiology* **166**, 492-500.

829